X-ray Variability of an Illuminated Irregular Accretion Disk around a Black Hole

Gang Bao and Paul J. Wiita
Department of Physics & Astronomy, Georgia State University,
Atlanta, Georgia 30303-3083
e-mail: bao@chara.gsu.edu; wiita@chara.gsu.edu

ABSTRACT

Models for active galactic nuclei and X-ray binaries where "cold" rotating matter is illuminated by a non-thermal source above it have been widely studied, and they successfully explain the main spectral features of black hole candidates, including reflection humps above 10 keV and the iron line at 6.4 keV. Making the reasonable assumptions that the innermost part of an accretion disk around a black hole is unstable and clumpy and that it is illuminated by X-ray sources originating above it, we compute the X-ray variability induced both by a clump of matter moving relativistically around the black hole and by the non-thermal source moving above the disk. One interesting new result we find is that even for a face-on geometry, rotation induced variability can still be observed as long as the non-thermal source is not exactly at the symmetry axis; this is true even if the accretion disk is smooth. We also show that the reflected X-ray component, peaked around ten or several tens of keV, can vary more than other spectral components, such as the thermal emission from the disk and the external power-law flux, and that it carries richer information on the non-thermal sources. This is because the reflected component experiences a double path through the gravitational field of the central mass, i.e., from the source to the disk, and then from the disk to the observer. Thus our study is most relevant to X-ray variability of black hole candidates where relativistic effects are strong. These results may provide a partial explanation of why some Seyfert 1 galaxies exhibit rapid X-ray variability with timescales comparable to the fastest orbital periods, and why soft X-rays and UV emission generally show slower variability than do the hard X-rays.

Subject headings: accretion, accretion disks — black hole physics — galaxies: active—galaxies: Seyfert — X-rays: general

1. Introduction

Current X-ray emission models of active galactic nuclei involve three main components: quasi-thermal emission from an accretion disk; direct emission from a power-law source; and power-law photons reprocessed/reflected by cold matter (e.g., in the accretion disk) (Guilbert & Rees 1988). These components are expected to be responsible for the spectral features such as absorption edges, fluorescent lines and a Compton reflection hump in the X-ray spectrum. Lightman & White (1988) gave an early detailed calculation of the reprocessed/reflected spectrum. They considered reprocessing of the X-rays by absorption and scattering in the cold matter, and predicted a broad "hump" of emission peaking at ~ 30 keV. The observed X-ray spectra of most Seyfert galaxies and some X-ray binaries show many significant features: a non-thermal power-law in the hard X-ray band; a "reflection hump" from 10 keV to 100 keV; and fluorescent lines around 6.4 keV (e.g., Mushotzky 1982; Malkan 1983; Arnaud et al. 1985; Turner & Pounds 1989; Pounds et al. 1990; Matsuoka et al. 1990; Turner et al. 1990). The temperature ($T \sim 10^5$ K for Seyferts) and the luminosity of this emission implies that there exist large quantities of relatively cold matter within the innermost region of AGN and in some X-ray binaries (e.g., Cyg X-1 with $T \sim 10^6$ K) which supports the models of Guilbert & Rees (1988), and of Lightman & White (1988).

This popular scenario involving essentially thermal rotating matter illuminated by a non-thermal source has so far mainly been applied to the study of the static spectral features of black hole candidates (e.g., Haardt & Maraschi 1993; Mushotzky et al. 1995; Nandra et al. 1997; Reynolds & Begelman 1997). Here we stress that these three components of X-ray emission of active galactic nuclei must also be the dominant sources of X-ray spectral and temporal variability. The fluctuations may reveal some important information which the spectral studies could not yield, e.g., on the scale and location of emitting sources. Currently, there exist numerous variability models such as shot noise (e.g., Roberto & McHardy 1989), and magnetic flares (e.g., de Vries & Kuijpers 1992, Chagelishvili, Lominadze & Rogava 1989; Di Matteo 1998), but none of them has incorporated the above framework for spectra.

In this paper we assume that the cold matter (dense clouds as mentioned by Guilbert & Rees 1988) is in the form of a "clumpy disk", which is illuminated by a non-thermal source above the disk. Several papers have concentrated on the physics of such relatively cold clumps embedded within a hotter material (e.g., Celotti, Fabian & Rees 1992; Kuncic, Blackman & Rees 1996). Krolik (1998) has recently developed a model of a clumpy accretion disk in which both the thermal properties of the clumps and overall equilibrium of the "clumpy" accretion disk are discussed. In equilibrium, where cold matter coexists with hot plasma, the majority of the mass around a black hole is in dense and cool blobs. Each blob is very optically thick to Compton scattering, so they are individually and collectively effective absorbers of soft X-rays and reflectors of hard X-rays, so Krolik's model adds support to the general picture we present here.

A clumpy model has also been used to study the property of X-ray emission lines by Bond & Matsuoka (1993). Haardt, Maraschi, & Ghisellini (1994) proposed a X-ray emission model of active galactic nuclei and black hole candidates by assuming that the X-rays emitted are dominated by Comptonization of the disk photons by localized blobs within the accretion disk. Our model takes the hard X-rays to arise from an external source above the disk while the blobs emit thermal photons and reflect those hard X-ray photons. Both spectral and temporal variability of this model are investigated here. The innermost part of an accretion disk is subject to a number of well-known instabilities (Lightman & Eardley 1974; Shakura & Sunyaev 1976), so much of the radiation probably does not arise from a continuous medium, but rather from discrete blobs of matter which move relativistically around the central black hole. The observational data in the X-ray band support both aspects of this disk hypothesis: the chaotic X-ray lightcurves of black hole candidates imply that the innermost region close to the black hole is not smooth but, rather, clumpy; the observed iron line profiles are often found to be in good agreement with those expected to form in the inner regions of accretion disks around black holes (Mushotzky et al. 1995; Tanaka et al. 1995; Fabian et al. 1995; Nandra et al. 1997). Specifically, the width and the profile of the fluorescent iron line of both Galactic black hole candidates (e.g., Cygnus X-1, Fabian et al 1989) and active galactic nuclei (e.g., MCG 6-30-15, Tanaka et al. 1995) are interpreted as arising from large Doppler and gravitational shifts when accreting matter orbits the central black hole (Fabian et al. 1989; Pounds et al. 1990). This suggests that the accreting matter should not be at "rest".

The resulting clumps of thermal matter may still have roughly the same thickness and density as would the standard accretion disk, which satisfies the condition for "cold" matter (Lightman & White 1988; Krolik 1998). Also, as the central region near the BH is quite dynamic, non-thermal sources above the disk will probably not be static either. They could move: essentially along the axis perpendicular to the disk plane (for example, a shock in a jet); in an essentially orbital fashion (for example, a flare attached to, but above the disk); or in a more irregular fashion.

Apart from providing a more general study of this class of variability model than has been attempted hitherto, our studies include double gravitational bending effects: both the paths of the photons from the X-ray source(s) falling onto the disk clump and the paths of outgoing photons reflected by the clumpy region of the accretion disk are affected by general relativity, but the former factor has not been considered previously in this context. Reynolds & Begelman (1997) have considered these double bending effects by an X-ray source located on-axis and close to the disk when modeling the shape of the iron line. Bao, Wiita & Hadrava (1998, hereafter Paper I) have explored this relativistic effect on the gross shape of the spectra when the source of the illumination is at an arbitrary location but far enough away that the incident X-ray photons can be considered to provide a parallel beam, illuminating the entire disk. In this scenario, the reflected photons extract both energy and angular momentum from the relativistically rotating accretion disk and are beamed in the direction of the disk velocity. The influence of this effect can be crucial in some special situations (Paper I). Also, since the double-path is only associated with the reflected component of the non-thermal source, the resulting reflection hump and its variability are sensitive indicators of the geometry of the power-law source. Here we build upon our earlier work to investigate both the spectrum and the flux variability due to the relativistic rotation of a clump in an equatorial orbit as well that arising from different locations of the power-law X-ray source. In §2 we describe the method of the calculation and give the numerical results in §3; §4 comprises a discussion and conclusions.

2. The Relativistic Model

As mentioned above, the high energy spectral features of Seyfert galaxies are usually interpreted in terms of a model in which the primary X-ray power-law continuum is reflected from and reprocessed in an accretion disk. Fig. 1 shows the geometry considered; i_1 and i_0 are respectively the inclination angles of the observer and the X-ray source to the symmetry (disk angular momentum) axis, and Δ is the orientation of the non-thermal source relative to the observer (defined so that $\Delta = 0$ if the source and observer are on the same side of the axis). For a clear view, we show a situation where the clumpy disk is illuminated by the non-thermal X-ray source when it is sufficiently far away to provide effectively plane parallel illumination; all the parameters labeled are the same for non-parallel radiation cases, and an additional distance from the origin then defines the location of the non-thermal source.

The X-ray photons coming from the non-thermal source will be gravitationally shifted and Doppler shifted (depending on the relative motion of the non-thermal source and the accretion disk) on their route to the disk, and will be shifted again after the "reflection" from the clump towards the observer at infinity. The quasi-thermal photons coming directly from the accretion disk will be affected only once (as has been considered previously by many authors, e.g., Fu & Taam 1990; Hollywood & Melia 1995). Also, if the inclinations to the disk normal of both the source and observer are high, then the external X-ray photons will experience significant double bending before they reach the observer, but the thermal photons are bent only once.

Our approximation to the observed spectrum contains three components: the non-thermal radiation coming directly from the X-ray source, the radiation from the blob in the accretion disk, and the radiation reprocessed by the clumpy accretion disk, which comprises effectively cold matter as far as the X-rays are concerned. This condition for cold matter requires that the disk should be radiating substantially below the Eddington limit ($L \lesssim 0.1 L_{\rm Edd}$) (Matt, Fabian & Ross 1993; Nandra et al. 1995) which is certainly satisfied for the specific sets of parameters we consider below.

In its rest frame the power-law X-ray component is expressed by $I_{E,p} = C_1 \; E^{-\alpha} \exp(-E/E_{cut})$, where E_{cut} is the effective upper cut-off energy of the spectrum, typically set to 100 keV in our work, and $C_1 \; = E_{min}^{\alpha} \exp(E_{min}/E_{cut})$, where E_{min} is the minimum energy considered and is taken as 0.05 keV. We compute the blob's emission spectrum in its rest frame using the standard prescription for thin α-viscosity accretion disks from Novikov and Thorne (1973); basically, this spectrum is a sum of modified black bodies, and for any given radius, $I_{E,d} = C_2 \; E^3/\{\exp[E/kT(r)] - 1\}$. This is obviously an approximation for a clumpy disk and thus the detailed spectra presented below are not exact; however, we note that the surface temperature of the clumps as estimated by Krolik (1998) scale similarly with radius, mass and accretion rate as do the standard thin disk temperatures, with the normalization depending only weakly upon the effective viscosity parameters for the clump and hot-disk regions. Thus, the spectral differences between smooth and clumpy disks, at least at the lower energies where direct radiation from the disk dominates, should not be too large, and will not affect our basic results. The ratio of the power-law plus reflection components to the disk component are adjusted using C_2 so that both can be comparable in the figures. Generally, we choose C_2 to be between 4×10^2 to 4×10^4. The final component is the "reflected" spectrum which is computed similarly to Lightman & White (1988); this scenario assumes that the non-thermal source illuminates the cold blob matter, and it is then reprocessed by this matter through atomic absorption and electron scattering. We employ a program kindly provided by F. Haardt to calculate the reflected components. For details see Paper I.

Define $I_{\nu_{em}}$ as the local specific intensity at frequency ν_{em} at the disk and $I_{\nu_{ob}}$ the intensity observed at frequency ν_{ob} at infinity. The generalization of Liouville's theorem (e.g., Misner, Thorne & Wheeler 1973), means that if $f(\mu)$ is a direction dependence function, which is determined by the local physics of scattering (Paper I) their relation can be written

$$I_{\nu_{ob}} = g^3 I_{\nu_{em}} f(\mu) \qquad \text{ergs cm}^{-2}\ \text{s}^{-1}\ \text{Hz}^{-1}\ \text{sr}^{-1}, \tag{1}$$

where the total frequency shift at a point (r, φ_s) on the disk is defined as the ratio of the observed energy of a photon to that of the emitted energy (measured at the local frame), $g = E_{ob}/E_{em}$. This g factor includes both the gravitational shift and the Doppler shift (from disk rotation), and is given by (cf. Bao 1992)

$$g = \frac{[(1-v_s^2)(1-2/r)]^{1/2}}{1-\Omega L_z}, \tag{2}$$

where Ω is its angular velocity, $v_s = \Omega\, r\, (1-2/r)^{-1/2}$ is the velocity of the emitting matter measured in the local static frame, and L_z is the component of its angular momentum about the z (symmetry) axis; the angular dependence of the redshift factor g is embedded in L_z. Spherical coordinates and the geometric units in which $G = c = 1$ are used, and for simplicity, dimensionless physical quantities are employed.

Therefore, the observed spectrum can be written as

$$F_{\nu_{ob}} = \int I_{\nu_{ob}} d\Pi \ \ \mathrm{erg\ cm^{-2}\ s^{-1}\ Hz^{-1}}, \tag{3}$$

where Π is the solid angle the emitting matter subtends at the observer; this directly measures the bending or lensing effect. In terms of the total impact parameter B and the position angle ϕ' of the photon, $d\Pi = BdBd\phi' D^{-2}$, where D is the distance between the observer and the emitting matter; $d\Pi$ can be rewritten in terms of the coordinates of the disk, r and φ_{s}. Bao, Hadrava, & Østgaard (1994) provide the methods used here to calculate the solid angle and the impact parameter.

Equations (1)–(3) can be used directly to calculate the observed spectrum of the thermal radiation from the blob in the accretion disk, but $I_{\nu_{ob}}$ needs to be expressed in terms of the specific intensity of the power-law source I_{ν_p}, and thus a more difficult computation must also be performed. This is because thermal photons come from the disk directly and we can use formula provided by Novikov and Thorne (1973), while the reflected X-ray photons come first from the source to the disk and then from the source to the observer. Apart from the relative motions between the observer and a portion of the accretion disk, there also exists relative motion between the non-thermal source and the accretion disk segments. According to equations (1) and (2), the power-law specific intensity measured *on the disk* will be inversely proportional to the redshift factor to the third power and the solid angle at infinity, and therefore the reflected intensity measured by the observer at infinity will be proportional to the ratio of the redshift factor for the outgoing photon (g_1) to that of the incoming photon (g_0) to the third power and the ratio of the solid angle for the outgoing case to that for the incoming case. For an area element of Δs on the disk, which has solid angles $\Delta\Pi_0$ and $\Delta\Pi_1$ subtended at the source and the observer respectively, we have

$$I_{\nu_{ob}} = I_{\nu_p}\Big(\frac{g_1}{g_0}\Big)^3 \frac{\Delta\Pi_1}{\Delta\Pi_0}. \tag{4}$$

Clearly, the impact parameters B of the incoming and outgoing X-ray photons are different, and must be calculated independently, i.e., for one blob or small element of the disk one has to calculate two impact parameters: one for the incoming path and the other for the outgoing path. The impact parameters depend on the location of the element (r), the viewing angles of the non-thermal source and the observer (i_0, i_1), the distance of the power-law source to the element and the orientation of the source relative to the observer. These make computing the observed reflected spectrum quite complex, even for our simplifying assumptions of a non-rotating black hole and a single clump. A point worth bearing in mind is that when calculating the outgoing path, one can always assume the observer is at "infinity", in that the observer is so far away that the gravity of the black hole has little influence on the path of photons around the observer. However, a power-law source can be at "infinity" or it can be reasonably close to the black hole. When it is close to a black hole, some of the parameters in the formulae of previous papers (e.g., Bao, Hadrava & Østgaard 1994), on which the calculations of this paper are based, should be changed. Most importantly, the factor

$$\int_0^{u_s} \frac{du}{\sqrt{2u^3 - u^2 + B^{-2}}},$$

will be changed to

$$\int_{u_p}^{u_s} \frac{du}{\sqrt{2u^3 - u^2 + B^{-2}}},$$

where $u = m/r$, u_s corresponds to location of the disk's element, and u_p to the location of the power-law source. One must consider turning points on the paths so that some integrations are not ignored.

3. Numerical Results

All of the following illustrative calculations have assumed a blob drawn from a relativistic disk around a $10^6 \mathrm{M}_\odot$ black hole with an accretion rate of 0.01 $\dot{M}_{\mathrm{Edd}}$ and $\alpha_{\mathrm{vis}} = 0.01$.

Fig. 2 shows the spectrum variability for the reprocessed component alone where this component is dominated by a single clump. The non-thermal source is assumed to be far enough away to be treated as providing parallel rays at phase $\Delta = 0°$, and the clump orbits the black hole at radius $r = 10m$. Variability is clearly seen when the clump is at different locations. The maximum amplitude of the spectrum (long-dashed line) corresponds to the the case when the clump moves towards the observer and the minimum (dotted-line) to the case when it moves away from the observer. There are two factors playing a role here. First, the Doppler effect, which is well known. Second, the non-thermal photon obtains energy from the relativistically rotating disk, a process similar to inverse Compton scattering. The non-thermal photons extract energy from the rotating clump and are beamed in the direction of the disk's local velocity, an effect that is produced for photons reflected by a rotating object. Thus, this aspect of amplitude and spectral variability depends very much on the location of the observer, the location of the non-thermal source, and the location of the clump. In Fig. 3, we present the variability of the reflected component for parameters different from those of Fig. 2, and we see that the variability pattern is amplified for a larger angle to the source of incident photons. It is important to note that in both these cases the disk has a face-on geometry, but the observer can still see the rotation induced variability. This is quite a different result from the case of direct emission (Abramowicz et al. 1989; Zhang & Bao 1991; Wiita et al. 1991; Mangalam & Wiita 1993; Bao et al. 1994) but should not be surprising because the difference arises from the non-thermal source being off the symmetry axis (also see §4).

Fig. 4 displays the light-curve for the reflected X-ray at three different energies, i.e., $E = 1$, 5, and 10 keV, for a single reflected clump. These curves are not very different from what was seen earlier arising from individual emitting blobs (e.g., Cunningham & Bardeen 1973; Bao 1992). The peaks correspond to the cases when the clump is right behind the black hole, so that the reflected photons are focused strongly when viewed at large inclination angles ($i_1 = 85°$ here).

Fig. 5 and Fig. 6 show variations of the total spectra which include all three components: power-law (coming directly from the non-thermal source), the modified black body (originating from the clump in the disk), and the reprocessed radiation (first impacting the blob from the non-thermal source, then reprocessed and reflected). In both cases we have $\Delta = 0°$. In Fig. 5, the parameters $i_1 = 40°$, $i_0 = 50°$, and $r = 20m$ are used. In Fig. 6, the only changed parameters are $i_1 = 1°$, and $r = 10m$. We see variability for both the disk component and for the reflected component in Fig. 5. In this case, the variabilities of these two components are quite similar: the largest amplitude corresponds to the clump at 270° (approaching) and smallest amplitude to the clump at 90° (receding). But one should note that this similarity in structure with phase is not always true, because both components have very different experiences in their paths through the gravitational field. This is seen in Fig. 5 where the disk's component at $\phi = 0$ is exceeded by the focused emission at 90°, but the reflected component at $\phi = 0$ is greater than that at 90°. This difference in variability is best expressed by Fig. 6 which shows a large variability amplitude in the reflected components while there is essentially no variability in the disk component because of the different paths the direct and reflected photons traverse. When the orbit of the cold matter is effectively face-on, one observes no rotation effect for the thermal photons coming directly from the clumpy disk; however, since the non-thermal photons come first from the power-law source (which has a inclination of 50° in this case) and are then reflected by the blob, variations are seen in the reflected component. This phenomenon may have been observed, as will be discussed in the next section.

In the above calculations, we studied situations where cold matter is illuminated by parallel rays of photons, implying that the non-thermal sources are effectively at infinity. Figs. 7 and 8 show the results of cases when the non-thermal source is effectively point-like and located at various distances from the central BH along different directions. As expected, the intensity of the reflection hump decreases when sources move away from the disk and increases when the sources approach the disk. Fig. 9 presents the composite spectra with the non-thermal source being at $6m$, $8m$ and $20m$. The reflection humps vary as shown in Fig. 8, but there are no changes in the disk components. This is because the disk spectrum is effectively independent of the X-ray source location in our current considerations.

In Fig. 10 and Fig. 11 we show situations where either the source or the reflecting blob changes its phases while keeping other parameters fixed. In Fig. 10, both source and the blob are at $r = 10m$, with $i_0 = 40°$, $i_1 = 20°$, and $\Delta = 0°$; we show what would be seen as the blob moves in a circular orbit. Variability of the disk component is obvious: we see the maximum amplitude of the spectrum when the blob is moving towards us (blueshift) and the minimum amplitude when it recedes from us (redshift). The reflected component behaves differently from that coming directly from the clump, as the distance (r_p) between the source and the blob plays a crucial role. The maximum amplitude corresponds to the case when the blob is at $\phi = 0$, where r_p is the smallest. Second to the maximum is the case where the blob is at $\phi = 270°$. Although r_p is the same for $\phi = 90°$ and $270°$, in the case $270°$ we have $g > 1$ while in case $90°$ we have $g < 1$, which explains why their amplitudes are different. In Fig. 11, no variability is seen in the disk component, but only in the reflected one. This is obvious because the blob's location has been fixed and the thermal component comes from the non-varying disk. Again, r_p plays a crucial role in the differences among the humps. The r_p for long dashed line is the smallest (with $\phi = \Delta = 270°$) and the dotted line corresponds the largest r_p ($\phi = 90°$). Other cases are mediated by differences in g's. It should be mentioned that even if the blob has no motion it does not mean the redshift factor has no role in producing variability, even though that is true for the disk component alone. Because of the relative motion between the source and the blob we have a varying g_1 around unity. Thus, the observer can still detect the the motion of the source through the “mirror” of the reflecting disk.

4. Discussion and Conclusions

Currently, the model involving non-thermal sources illuminating an accretion disk is widely accepted. This is because it can naturally explain many observed data (see §1 and Paper I), especially features of the spectra of both AGN and galactic black hole candidates. Operating within this framework, we have demonstrated how spectral and temporal variability can be induced through disk and source motions.

We have aimed at understanding the X-ray spectrum and flux variability of an illuminated clumpy disk. Although we explicitly investigated the variability arising from reprocessing by a single clump, the basic properties of an ensemble of the clumps may be deduced from the results obtained here. To do so, one can use insights gained from our earlier work on temporal variability produced by a large group of directly radiating spots (e.g., Abramowicz et al. 1989; Bao 1992; Mangalam & Wiita 1993; Bao et al. 1994). While distinct orbital signatures can be washed out, variability will be detected at a wide range of frequencies. The most interesting new result we find now is that even when an accretion disk has a face-on geometry, one can still observe the rotation effect and thus the rotation induced variability. This is because some of the observed X-ray photons have two different paths through a strong gravitational field, first, from the non-thermal source to the disk, second, from the disk to the observer.

Let us examine how this works. Suppose g represents the redshift factor, which is defined as the ratio of the energy measured at infinity to the energy measured at the local frame. In our case, the local frame is set on an element of accretion disk. Let I_s, I_d, and I_o be the frequency integrated intensity of the radiation at the source, disk and observer, respectively. The observed total intensity, $I_o \propto I_d\ g_o^4$; the extra power of g here compared to Eqn (1) for specific intensity arises from the integral over ν. The local illuminated total intensity, $I_d \propto I_s\ g^{-4}$; so, we have $I_o \propto (g_o/g_s)^4$. For simplicity, we discuss the Newtonian case where we have

$$g = 1 - \frac{v}{c} \sin i \sin\phi,$$

so that

$$I_o \propto \Big[\frac{1 - \frac{v}{c}\sin i_1 \sin\phi}{1 - \frac{v}{c}\sin i_o \sin(\phi - \Delta)}\Big]^4, \tag{5}$$

where v is the velocity of the clump and ϕ is the orbital phase of the clump. We see clearly that even when the observer is on the symmetry axis, i.e., $i_1 = 0$ ($g_o = 1$), as long as i_0 is not zero, then I_o will still be affected by the rotation effect, i.e.,

$$I_o \propto \Big[1 - \frac{v}{c}\sin i_o \sin(\phi - \Delta)\Big]^{-4}.$$

A full relativistic consideration of this factor, as was performed in our numerical computations, will include gravitational shifts and lensing, but the above conclusion is general.

This phenomenon is clearly relevant to the X-ray variability, especially the reflected component ranging from 10 keV to several tens of keV, because the thermal photons come directly from the disk, which experience a single path, while many non-thermal high energy photons reach the observer through double paths. Within the now commonly accepted unified scheme for AGN (e.g., Antonucci 1993), the Seyfert 1 galaxies are viewed at relatively low inclinations, $i_1 < 45°$, while Seyfert 2's are observed from greater inclinations and their central regions are obscured by molecular tori. A direct prediction from our computations and the above discussion is that, for Seyfert 1's, we could always expect to observe rapid variability with shortest timescales corresponding to blobs in the inner disk region, even though some may have an essentially face-on geometry ($i_1 \sim 0°$). A second prediction is that the soft X-ray and UV emissions have slower variability compared to the hard X-rays. According to our model, the rotation induced variability makes a substantially smaller contribution to the soft X-ray and UV variability if the system has a close to face-on geometry, as do the Seyfert 1's. Essentially all of the soft X-ray and UV photons only follow the direct route from the disk to the observer, so the redshift factor affecting them, $g \simeq 1 - \frac{v}{c} \sin i_1 \sin\phi \approx 1$, (for small i_1), implies there is little or no rotational induced variability. We note that some recent models (e.g. Sincell & Krolick 1997) have argued that much of the UV continuum in AGN may also come from reprocessing and reflection; if this is so, then our claim of different sources of variability in different bands is weakened.

It is well known that rapid and chaotic variability is common in the X-ray emission of AGN, including Seyfert 1's. The variability spectra of most AGNs are characterized by a nearly featureless power-law dependence on variability frequency, i.e., $p(\omega) \sim \omega^{-\beta}$ with the power index being around $\beta = 1.55$ (Lawrence & Papadakis 1993) within the frequency range $10^{-5} - 10^{-3}$ Hz (Pounds & McHardy 1988). Generally, the observed low-energy power spectra are steeper than the corresponding higher-energy ones (e.g., McHardy 1989), suggesting the hard X-ray emissions vary more on short timescales. The variability timescale due to motion of blobs in an accretion disk is related to their orbital periods. The shortest timescale within the orbiting model is introduced by blobs at the last stable orbit. For a slowly rotating black hole with mass M, a rotation induced variability timescale could exist down to

$$T = 12\pi\sqrt{6}M = 4.6 \times 10^4 m_8 \text{ s},$$

(G and c are set equal to unity) where m_8 is the mass of the central black hole in units of $10^8 M_\odot$. So, for AGN black holes with masses $10^6 - 10^9 M_\odot$ this type of variability timescale can be minutes to days, which is consistent with the observations. Recent *ASCA* observations of the Seyfert 1 galaxy IRAS 18325-5926 appear to show a substantial variation with a periodicity of 5.8×10^4s (Iwasawa et al. 1998), although many faster (non-periodic) variations were also seen. The possibility that claimed periodicity is related to orbital motion of a long-lived flare or bright clump was considered by those authors to be the most likely explanation. This certainly could be accommodated within our model as arising predominantly from clump motion, which would set an upper limit to the mass of a Schwarzschild BH of $\sim 1.3 m_8$. The folded light-curve presented by Iwasawa et al. (1998) appears rather sinusoidal, so that gravitational lensing effects are not predominant; this suggests that the inclination angle is $< 60^\circ$ (cf. Bao 1992), which is in agreement with those authors' estimate that it is $\sim 50^\circ$.

Our model suggests that the reflected X-ray component often varies more than the other components we have considered (disk and direct power-law); this should be the case if the clumps are very close to the central black hole, where the instabilities are expected to be strongest. Since the reflected X-ray energy usually peaks around 10–30 keV, the variability in this range will be most interesting. This variability carries rich information not only on the geometry of the disk but also on the geometry of the power-law X-ray source.

The above arguments could provide an important part of the explanation for the rapid hard X-ray variability of Seyfert 1's, and for the slower variability in their soft X-ray or UV bands (McHardy 1989). Obviously, there exists intrinsic variability in Seyferts and other AGN, but this intrinsic variability will probably not carry as much information on some important parameters, such as the mass of the black hole, the inclination of the system, and the geometry of the non-thermal sources. Once the intrinsic variability is modulated by the rotation effect, we have the opportunity to deduce (or at least constrain) these parameters.

Previous studies (either of X-ray spectra or of X-ray time variability) have confined their considerations to the general relativistic effect and the rotation effect on the path from disk to the observer only. This may seem appropriate when the disk is not nearly face-on; however, we have shown that this limitation can lead to wrong conclusions if the disk's inclination to the observer is close to zero. So, as long as the power-law sources of X-rays are not exactly on the symmetry axis (in many models they are scattered above the disks in the form of flares in a corona, e.g., Di Matteo 1998, and references therein), the observed X-ray fluctuations will continue to be modulated by the rotation of the disk, even when the disk is face-on to the observer. Contrary to our previous concept (Abramowicz et al. 1989; Zhang & Bao 1991; Mangalam & Wiita 1993; Chakrabarti & Wiita 1993), the rotational modulations of the "hot spot" model apply not only to those objects making a substantial inclinations to the line of sight, but also to many of those with face-on geometries.

Apart from purely intrinsic fluctuations and the rotation induced variability, another source of temporal variability in AGNs could arise from the motions of the non-thermal sources themselves. This aspect of the scenario is realistic because the X-ray sources close to a black hole are unlikely to be static. A recent study by Reynolds and Fabian (1997) investigated the motion of the X-ray source above an accretion disk and showed that relative motion between the disk and X-ray emitting material can have an important influence on the observed equivalent width of the iron line via relativistic aberration and Doppler effects. This may explain why the observed equivalent width of the iron line often exceeds the prediction of the standard X-ray reflection model. The relative motion between cold material and the X-ray source will introduce both line or spectrum variability and pure temporal variability. Unlike the predominantly orbital motions of the cooler clumps, motions of the primary X-ray sources may be irregular and difficult to distinguish within the observational data. This is simply because the physics behind these source regions is poorly known and many specific assumptions would need to be made to produce a model. Even if the primary source is located within a jet, which is presumably close to the symmetry axis (e.g., Reynolds & Begelman 1997), shock or bulk fluid motions away from the BH would yield changes in what we observe. In the case where the primary source is concentrated in a few flare-like regions above the disk (e.g., Di Matteo 1998) there could be variations induced by possible rotation of those flaring regions (if they are reasonably anchored to the disk below), but clearly vertical (and possibly even radial) motions during the course of flaring events would also change both the intrinsic intensity of the primary source as well as the distance and direction from which it illuminates the disk. Only if the primary emission region is rather smoothly distributed in a corona would variability induced by its motions be likely to be negligible. The key difference in variability between parallel and non-parallel illumination is that the former does not depend on the distance between the the reflecting parts of the disk and the non-thermal source, while the later does.

As we mentioned earlier, the cold matter behaves like a “mirror”, through which one may be able to determine if the power-law source is moving or static. The geometric property of the “mirror” system is described by the ratio of the redshift factors, g_1/g_0, and neither of them can be ignored. If g_0 is ignored (e.g., let $g_0 = 1$), one cannot “observe” the motion of the primary X-ray source in the reprocessed emission; in some geometries, the direct high-energy emission could be obscured, so this would be the only way to discover its motion. Obviously, if g_1 is ignored (e.g., let $g_1 = 1$) one can not “observe” the rotation of blobs (or disk). This “mirror” property may be worth investigating in some related contexts, such as variations in the intensity and profile of the K_α line. Note that this phenomenon is not limited to the case that cold matter appears as clumps, the blobs discussed above; it is also true even if the cold matter is perfectly smooth. How can we distinguish the variability of the source and that of the "mirror" (cold matter) itself? As the accretion disk is rotating, rotation induced variability is most likely present. But if the cold matter is essentially face-on then its rotation induced variability will not be observed. In this case the observed variability should be dominated by contributions from the intrinsic variations of the disk and the motion induced variability of reprocessed photons from the non-thermal source. Such motion induced variability has specific patterns: the reflection hump will increase (decrease) with time as the source approaches (recedes from) the disk; or it could be quasi-periodic (if the source has an orbital or helical motion). Most probably, there exist mixed motions, but the source of the variability pattern may be distinguishable from sufficiently good data. Seyfert 1's are probably the best candidates for this study, because statistically, there are many objects having effectively face-on geometries in this class. Information derived from these data could help us understanding the dynamics of the power-law sources if only one or a few of them dominate at any particular time.

Naturally, there might be many blobs on the disk plane at a given time, rather than the single one for which the computations presented here were performed. The presence of many blobs of comparable emissivity will smear out any specific variability pattern produced by a single blob, and will reduce the overall amplitude of variations, but the three main results we present in this paper would remain valid. First, for disks with a face-on geometry we can still observe the rotation induced variability as long as the power law source or sources are not exactly on the symmetry axis. This fact does not depend on the the number of clumps in the disk, although the amplitude of such variations will be reduced and may become undetectable if there are many clumps at comparable radii and of comparable sizes and intrinsic emissivities. Second, statistically speaking, the reflected hard X-rays vary more than other components. Again, this has nothing to do with the number of blobs. Finally, the basic results obtained in the case of source motion above the disk will be correct for any situation. Note that if there are so many blobs at similar radii and temperatures that the disk behaves as a smooth disk then any variability related to the disk rotation will disappear, but the source-motion induced variability discussed above could still be detected.

Compared to the many detailed studies of essentially simultaneous spectra, which clearly have been extremely useful, time variability studies of different portions of the spectrum are "under-developed". So far, there is not enough data to allow adequate analyses of the short timescale variability of AGN spectra, but our approach shows that this should be a fruitful pursuit. A serious study of variability in different bands should at least be able to provide much of the same information as have the already performed spectral analyses, and can, in principle, give additional knowledge of the inner regions of AGN. Previous X-ray telescopes have not had the combination of sensitivity and spectral resolution that could allow these different types of variability to be discerned. The next generation of X-ray telescopes, e.g., *AXAF* and *XMM*, will provide substantially greater effective areas and spectral resolutions, but will be limited to energies of less than 10–12 keV. Thus, they will not allow clear measurements of the variations in the Compton reflected components which peak at higher energies, although they will reveal much about the disk components. The instrument that should enable the untangling of the source motion variations from those due exclusively to the disk, at least for brighter sources, is *Constellation-X*, for it has been designed to have substantial sensitivity out to over 40 keV as well as superb spectral resolution below 10 keV. Although the work reported here is clearly preliminary, we expect that this type of analysis can be developed substantially further, and we plan to do so. This effort could provide sensitive tools to determine some important astrophysical parameters.

We thank Dr. F. Haardt for the use of his reprocessing program, and the anonymous referee for several very helpful suggestions. This work was supported by NASA grant NAG 5-3098, and by a Research Program Enhancement grant at Georgia State University.

REFERENCES

Abramowicz, M. A., Bao, G., Lanza, A., & Zhang, X.-H. 1989, in Two Topics in X-ray Astronomy, ESA SP-296, ed. J. Hunt & B. Battrick (Noordvijk: ESA), 871

Arnaud, K. A., et al. 1985, MNRAS, 217, 105

Antonucci, R. R. 1993, ARA&A, 31, 473

Bao, G. 1992, A&A, 257, 594

Bao, G., Hadrava, P., & Østgaard, E. 1994, ApJ, 435, 55

Bao, G., Wiita, P., & Hadrava, P. 1998, ApJ, 504, 58 (Paper I)

Bond, I. A., & Matsuoka, M. 1993, MNRAS, 265, 619

Celotti, A., Fabian, A. C., & Rees, M. J. 1992, MNRAS, 255, 419

Chagelishvili, G. D., Lominadze, J. G., & Rogava, A. D. 1989, ApJ, 347, 1100

Chakrabarti, S. K., & Wiita, P. J. 1993, ApJ, 411, 602

Cunningham, C. T., & Bardeen, J. M. 1973, ApJ, 183, 237

de Vries M., & Kuijpers, J. 1992, A&A, 266, 77

Di Matteo, T. 1998, MNRAS, 299, L15

Fabian, A. C., Nandra, K., Reynolds, C. S., Brandt, W. N., Otani, C., Tanaka, Y., Inoue, H., Iwasawa, K. 1995, MNRAS, 277, L11

Fabian, A. C., Rees, M. J., Stella, L., & White, N. E. 1989, MNRAS, 238, 729

Fu, A., & Taam, R. E. 1990, ApJ, 349, 553

Guilbert, P., & Rees, M. J. 1988, MNRAS, 233, 475

Haardt, F., & Maraschi, L. 1993, ApJ, 413, 507

Haardt, F., Maraschi, L., & Ghisellini, G. 1994, ApJ, 432, L95

Lawrence, A., & Papadakis, I. 1993, ApJ, 414, L85

Hollywood, J. M., & Melia, F. 1995, ApJ, 443, L17

Iwasawa, K., Fabian, A. C., Brandt, W. N., Kunieda, H., Misaki, K., Reynolds, C. S., & Terashima, Y. 1998, MNRAS, 295, L20

Krolik, J. H. 1998, ApJ, 498, L13

Kuncic, Z., Blackman, E. G., & Rees, M. J. 1996, MNRAS, 283, 1322

Lightman, A. P., & Eardley, D. M. 1974, ApJ, 187, L1

Lightman, A. P., & White, T. R. 1988, ApJ, 335, 57

Malkan, M. A. 1983, ApJ, 268, 582

Mangalam, A. V., & Wiita, P. J. 1993, ApJ, 406, 420

Matsuoka, M., Piro, L., Yamauchi, M., & Murakami, T. 1990, ApJ, 361, 440

Matt, G., Fabian, A. C., & Ross, R. R. 1993, MNRAS, 264, 839

McHardy, I. M. 1989, in Two Topics in X-ray Astronomy, ESA SP-296, ed. J. Hunt & B. Battrick (Noordvijk: ESA), 1111

Misner, C. W., Thorne, K. S., & Wheeler, J. A. 1973, Gravitation (San Francisco: W. H. Freeman)

Mushotzky R. F. 1982, ApJ, 256, 92

Mushotzky R. F., Fabian, A. C., Iwasawa K., Kunieda, H., Matsuoka, M., Nandra, K., Tanaka, Y. 1995, MNRAS, 272, L9

Nandra, K., George, I. M., Mushotzky, R. F., Turner, T. J., & Yaqoob, T. 1997, ApJ, 477, 602

Nandra, K., Fabian, A. C., Brandt, W. N., Kunieda, H., Matsuoka, M., Mihara, T., Ogasaka, Y., & Terashima, Y. 1995, MNRAS, 276, 1

Novikov, I. D., & Thorne, K. S. 1973, in Black Holes, ed. DeWitt, C., & DeWitt, B. S. (New York: Gordon and Breach), 347

Pounds, K. A., Nandra, K. A., Stewart, G. C., George, I. M., & Fabian, A. C. 1990, Nature, 344, 132

Pounds, K. A., & McHardy, I. 1988, in Physics of Neutron Stars and Black Holes, ed. Y. Tanaka et al. (Tokyo: Universal Academy Press), 285

Reynolds, C. S., & Begelman, M. C. 1997, ApJ, 488, 109

Reynolds, C. S., & Fabian, A. C. 1997, MNRAS, 290, L1

Roberto G. A., & McHardy I. M., 1989, in Two Topics in X-ray Astronomy, ESA SP-296, ed. J. Hunt & B. Battrick (Noordvijk: ESA), 716

Shakura, N. I., & Sunyaev, R. A. 1976, MNRAS, 175, 613

Sincell, M. W., & Krolik, J. H. 1997, ApJ, 476, 605

Tanaka, Y., et al. 1995, Nature, 375, 659

Turner, M. J. L., & Pounds, K. A. 1989, MNRAS, 240, 833

Turner, M. J. L., et al. 1990, MNRAS, 244, 310

Wiita, P. J., Miller, H. R., Carini, M. T., & Rosen, A. 1991, in IAU Colloq. 129 Structure and Emission Properties of Accretion Disks, ed. C. Bertout et al. (Gif-sur-Yvette: Editions Frontières), 557

Zhang, X-H., & Bao, G. 1991, A&A, 245, 454

Fig. 1.— The geometry considered. Photons come from the source and are reprocessed and reflected by the orbiting clumps which also emit directly. In both directions the photons are shifted in energy and follow geodesics in the field of the central black hole. The inclination of the observer to the symmetry axis is i_1, and that of the source is i_0. The phase of the non-thermal source relative to the observer is Δ.

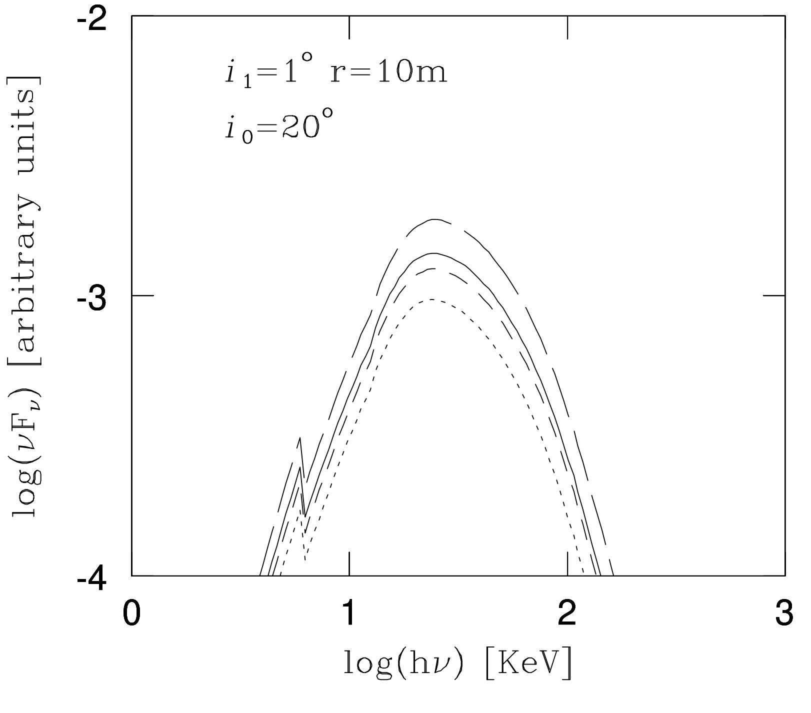

Fig. 2.— The spectral variability of the reprocessed component when the clump is at $r = 10m$ ($m = GM/c^2$), $i_1 = 1°$, $i_0 = 20°$ and $\Delta = 0°$. The clump moves from orbital phase 0° (solid line), through 90° (dotted line), and 180° (short-dashed line) to 270° (long-dashed line).

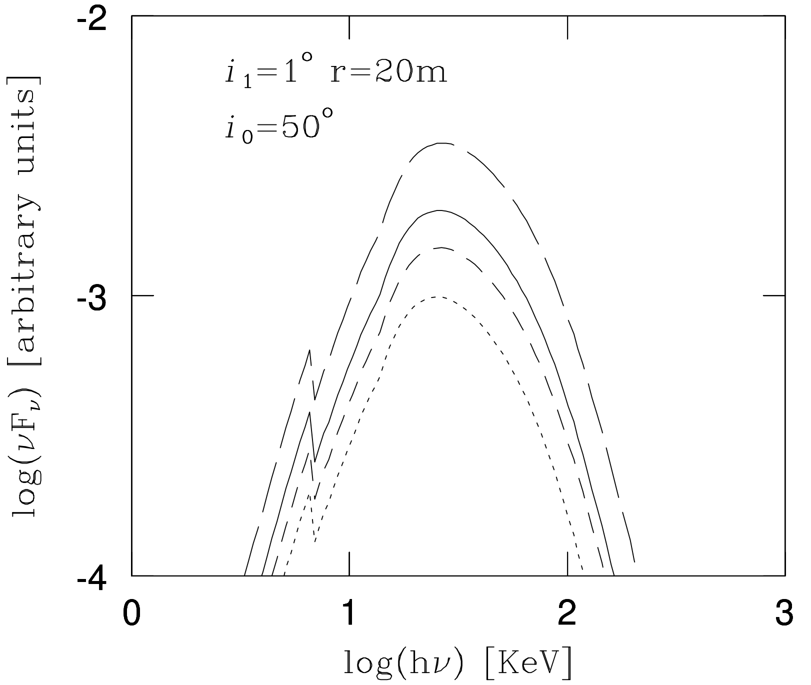

Fig. 3.— The spectral variability of the reprocessed component when the clump is at $r = 20m$, and $i_0 = 50°$. All other parameters are the same as in Fig. 2.

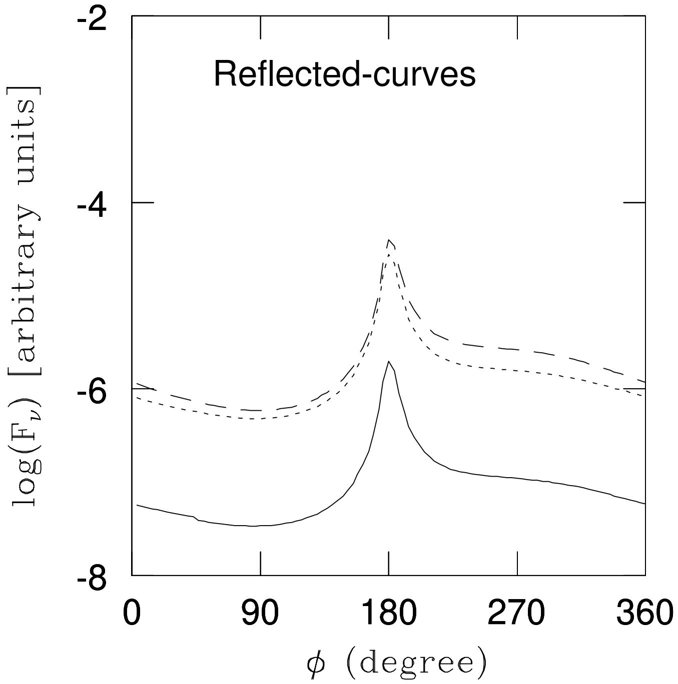

Fig. 4.— Light curve when a clump is at $r = 10m$, $i_1 = 85°$ and $i_0 = 20°$. The solid line refers to the curve of $E = 1$ keV, the dashed line to $E = 5$ keV, and the long-dashed line to $E = 10$ keV.

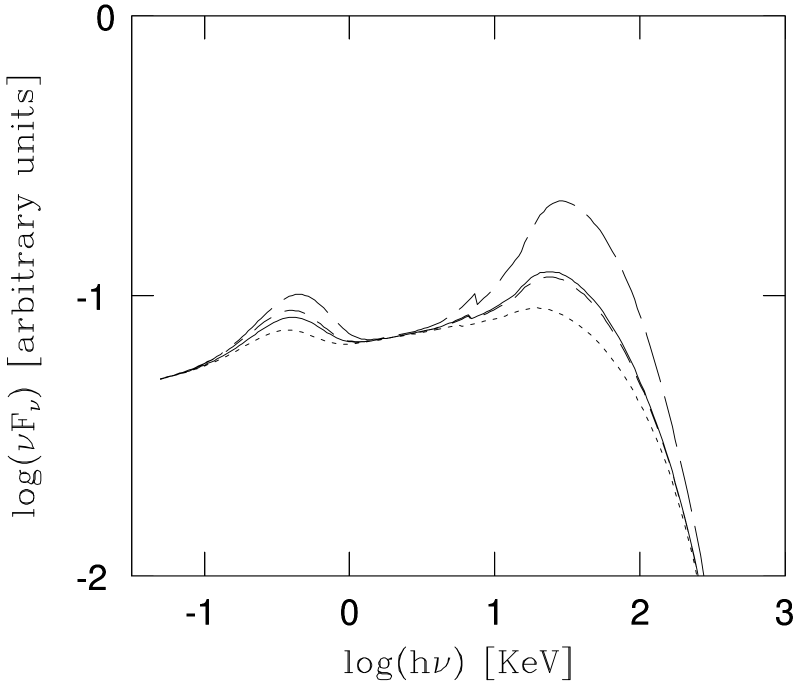

Fig. 5.— The composite spectral variability of the reprocessed, thermal and power-law components when the clump is at $r = 20m$, $i_1 = 40°$ and $i_0 = 50°$. The clump moves from phase 0° (solid line), through 90° (dotted line), and 180° (short-dashed line) to 270° (long-dashed line).

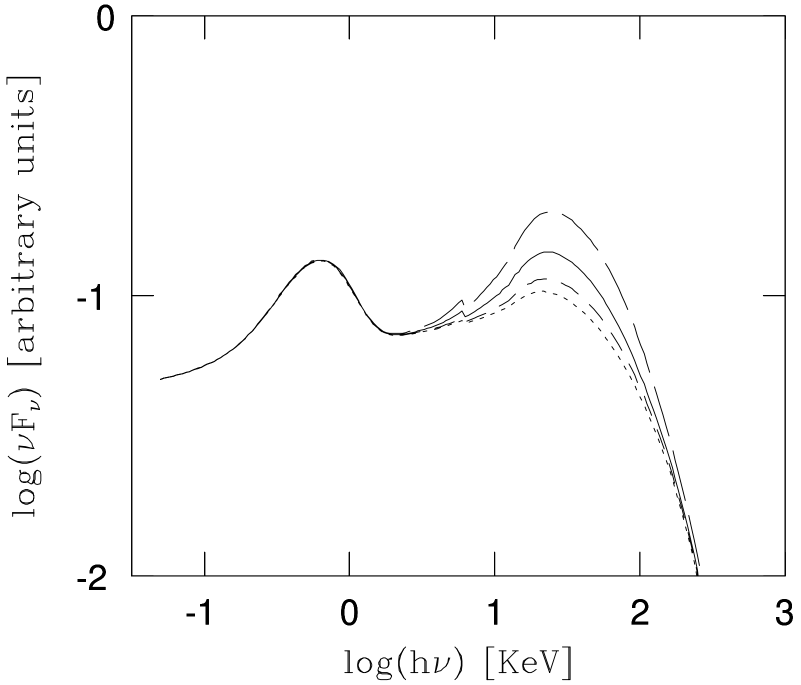

Fig. 6.— As in Fig. 5 except for $r = 10m$ and $i_1 = 1^{\circ}$.

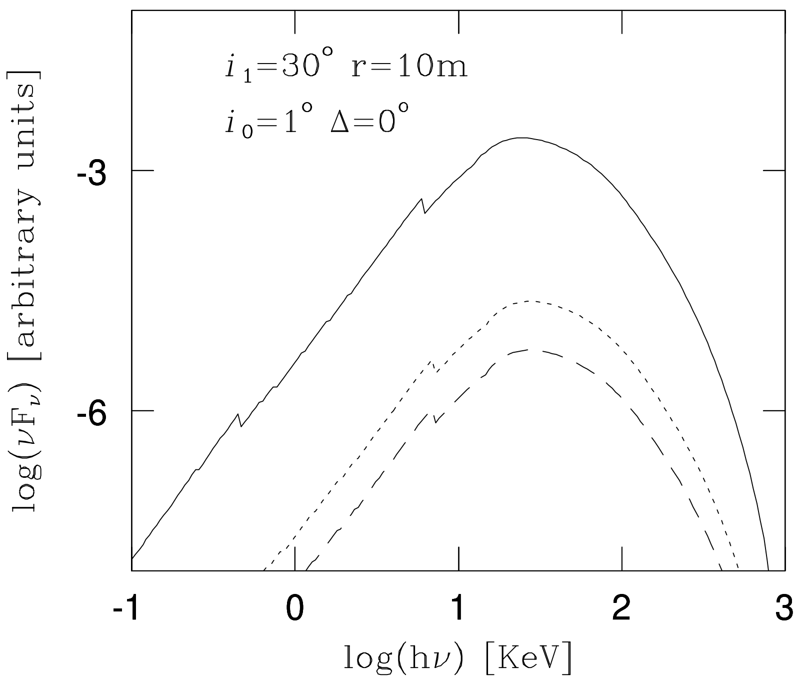

Fig. 7.— The spectral variability of the reprocessed component when a clump is at $r = 10m$ with the orbital phase $\Delta = 0°$ and $i_1 = 30°$, $i_0 = 1°$. The X-ray source with $\Delta = 0°$ has different distances to the central black hole: $10m$ (solid line), $50m$ (dotted line), and $100m$ (long-dashed line).

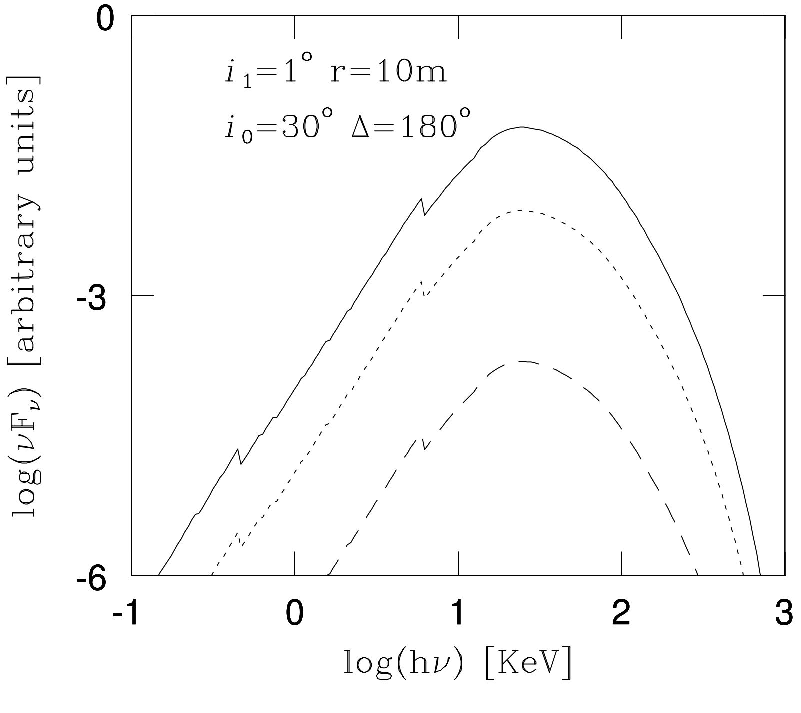

Fig. 8.— As in Fig. 7 but with $i_1 = 1^\circ$, $i_0 = 30^\circ$ and $\Delta = 180^\circ$.

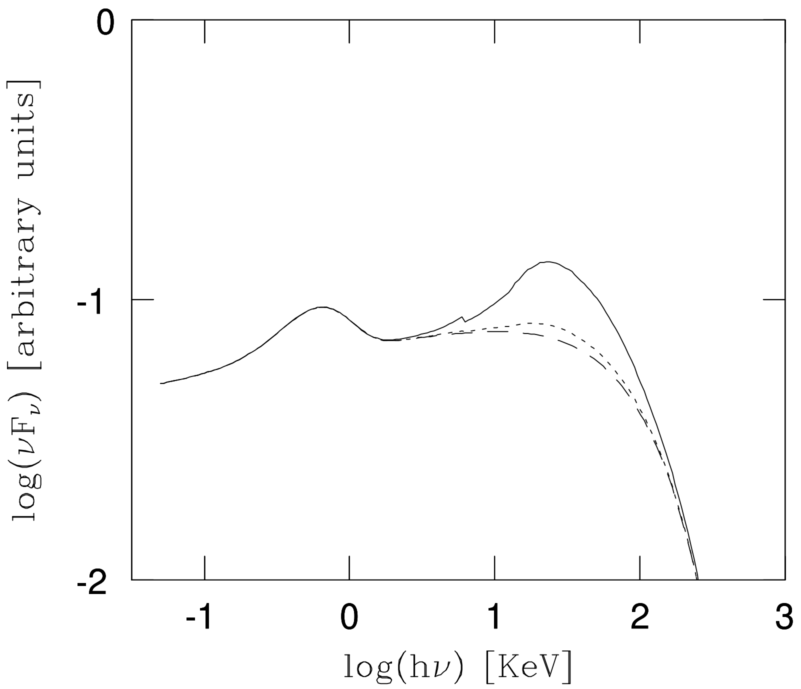

Fig. 9.— The composite spectral variability, including the reprocessed, thermal and power-law components. The solid line refers to the spectrum where the X-ray source is $6m$ from the central black hole, while the dotted line and long-dashed lines again correspond to distances of $8m$ and $20m$, respectively. All other parameters are the same as in Fig. 8.

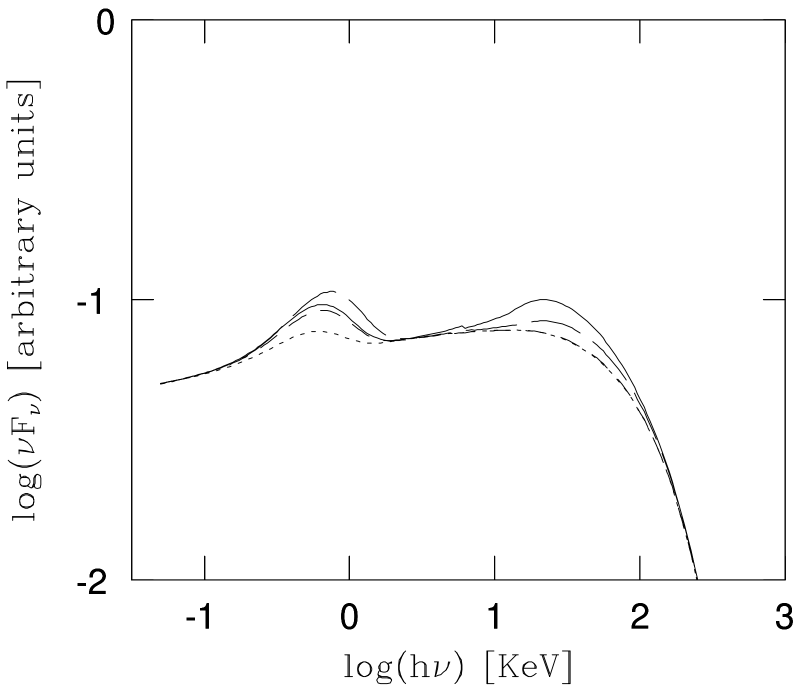

Fig. 10.— The composite spectral variability of the reprocessed, thermal and power-law components when both the clump and the source are at $r = 10m$, $i_1 = 40°$, $i_0 = 20°$ and $\Delta = 0°$. The clump moves from phase 0° (solid line), through 90° (dotted line), and 180° (short-dashed line) to 270° (long-dashed line).

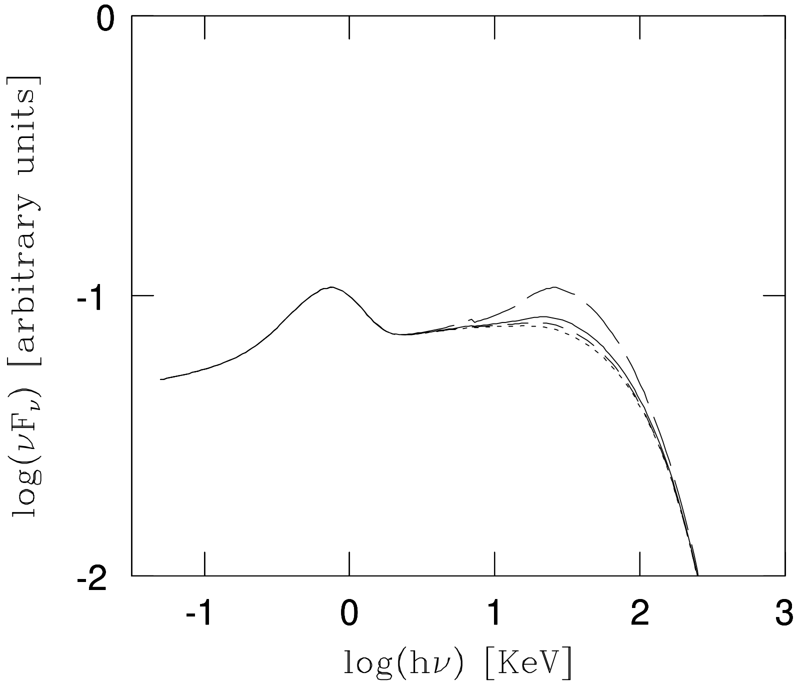

Fig. 11.— As in Fig. 10, except that now the clump is fixed at $\phi = 270^\circ$, while the source moves from phase 0° (solid line), through 90° (dotted line), and 180° (short-dashed line) to 270° (long-dashed line).